Published online 31 March 2011 *Nucleic Acids Research, 2011, Vol. 39, No. 14* ***5935–5944***
doi:10.1093/nar/gkr187

The relative efficiency of homology-directed repair has distinct effects on proper anaphase chromosome separation

Corentin Laulier, Anita Cheng and Jeremy M. Stark*

Department of Cancer Biology, Beckman Research Institute of the City of Hope, 1500 E Duarte Rd., Duarte, CA 91010, USA

Received February 15, 2011; Revised March 15, 2011; Accepted March 16, 2011

ABSTRACT

Homology-directed repair (HDR) is essential to limit mutagenesis, chromosomal instability (CIN) and tumorigenesis. We have characterized the consequences of HDR deficiency on anaphase, using markers for incomplete chromosome separation: DAPI-bridges and Ultra-fine bridges (UFBs). We show that multiple HDR factors (Rad51, Brca2 and Brca1) are critical for complete chromosome separation during anaphase, while another chromosome break repair pathway, non-homologous end joining, does not affect chromosome segregation. We then examined the consequences of mild versus severe HDR disruption, using two different dominant-negative alleles of the strand exchange factor, Rad51. We show that mild HDR disruption is viable, but causes incomplete chromosome separation, as detected by DAPI-bridges and UFBs, while severe HDR disruption additionally results in multipolar anaphases and loss of clonogenic survival. We suggest that mild HDR disruption favors the proliferation of cells that are prone to CIN due to defective chromosome separation during anaphase, whereas, severe HDR deficiency leads to multipolar divisions that are prohibitive for cell proliferation.

INTRODUCTION

Proper sister chromatid separation by a bipolar mitotic spindle is required to generate two identical daughter cells. During anaphase, all physical connections between sister chromatids must be resolved. For instance, cohesin complexes that link sister chromatids on the mitotic spindle need to be dissolved (1). Furthermore, since sister chromatids are intertwined (catenated) during DNA replication, sister chromatid separation requires decatenation via Topoisomerase II (2). Failure to resolve these sister chromatid linkages and/or maintain a bipolar mitotic spindle, can cause chromosomal instability (CIN) or cell death (3,4). Thus, characterizing the factors and pathways that are important for these aspects of anaphase will provide insight into genome maintenance.

Decatenation stress caused by catalytic inhibition of Topoisomerase II has revealed a set of distinct markers for incomplete resolution of sister chromatid linkages. Namely, decatenation stress causes bridges between anaphase chromosomes that can be identified by classic DNA dyes such as DAPI (5), but also ultra-fine bridges (UFBs) that are not detected by such dyes (6,7). These UFBs are readily detected by immunofluorescence staining for PICH (Plk1-interacting checkpoint helicase), which appears to associate with linked anaphase chromosomes that are under tension from the mitotic spindle (6,8).

A set of genome maintenance factors has been shown to promote resolution of these anaphase chromosome linkages. Cells deficient in the Bloom's syndrome helicase (BLM) show elevated CIN (9), increased sister chromatid exchanges (10) and an elevation in UFBs (8). Similarly, cells deficient in the Fanconi anemia pathway, which is critical for DNA interstrand crosslink repair (11), show cytokinesis failure, CIN and elevated levels of UFBs (12–14).

In this study, we characterize the impact of homology-directed repair (HDR) on proper chromosome segregation. HDR involves Rad51-mediated strand exchange between sister chromatids (15). Disruption of HDR factors is associated with increased mutagenesis, CIN, supernumerary centrosomes and cancer pre-disposition (16–20). As HDR is a major pathway of double-strand break (DSB) repair, disruption of HDR may cause an increased reliance on imprecise DSB repair mechanisms, such as non-homologous end joining (NHEJ), thereby causing increased mutagenesis (21,22). However, it is

*To whom correspondence should be addressed. Tel: +1 626 359 8111 (Ext. 63346); Fax: +1 626 301 8892; Email: jstark@coh.org

unclear how HDR deficiency also leads to CIN (18,23,24). Using the markers described above, we present evidence that HDR deficiency causes incomplete anaphase chromosome separation. Furthermore, we compare a mild versus severe HDR disruption and show that both degrees of HDR deficiency cause defects in anaphase chromosome separation, whereas, only severe HDR disruption leads to multipolar anaphases and cell death. We suggest that HDR-deficiency causes anaphase chromosome separation defects that can result in CIN, which could contribute to the etiology of cancer.

MATERIALS AND METHODS

Cell lines and culture conditions

The Embryonic Stem cell (ES cell) lines used in this study were previously described: $Brca1^{\Delta 11/\Delta 11}$ (21), $Brca2^{L1/L2}$ (25), ES^{KR} (26), $Xrcc4^{-/-}$ (27), $Xlf^{-/-}$ (28) and $Blm^{tet/tet}$ (29). ES cells were cultured on plates coated with 1% Gelatin (Millipore), in media containing DMEM High Glucose with 1% Pen/Strep, 15% Fetal Bovine Serum, 7×10^2 U/ml ESGrow (Millipore) and 0.1 mM β-mercaptoethanol (Sigma).

For inducible expression of Rad51, dominant negative proteins, Rad51-K133R and Rad51-K133A cDNAs (30) were cloned in the pNEBR-X1Hygro plasmid (New England Biolabs) and stably integrated into the HEK293A7 cell line that expresses regulator proteins from the pNEBR-R1 cassette (New England Biolabs). The 293 cells were cultured on plates coated with poly-lysine (Sigma), in media containing DMEM High Glucose with 1% Pen/Strep and 10% Fetal Bovine Serum. The +L condition reflects 1 μM Genostat ligand (L) (Millipore), where untreated media included the equivalent amount of vehicle, Dimethyl Sulfoxide (DMSO).

Quantitative RT–PCR

RNA was extracted using RNeasy Plus kit (Qiagen), reverse transcribed using random primers and MMLV-RT (Promega) and amplified with iQ SYBR Green Supermix (Biorad), each according to manufacturers instructions. Transcription from the g4Rad51 cassettes was measured by quantitative PCR using primers p1: ctggcgccaagcttctct and p2: cctcgacccgagtagtctgt. Signals were normalized to parallel PCR with actin primers: 5′-actgggacgacatggagaag, 5′-aggaaggaaggctggaagag.

Clonogenic survival and cell doubling time

Cells were seeded in 10 cm plates at 2×10^3 cells per plate in presence of L or left untreated, for 7 days. Colonies were fixed in 10% methanol, 10% acetic acid, stained with 1% crystal violet. Cell survival was calculated relative to the mean value of the untreated cells for each experiment. Each clonogenic survival value represents the mean of three independent experiments. For the cell doubling time measurement, 1.5×10^5 cells were plated and L was added the next day. Viable cells counts were performed over the next 3 days using a phase hemocytometer (Hausser Scientific) with trypan blue exclusion (4 mg/ml).

HDR assay

The HDR-reporter, Pim-DRGFP, was stably integrated in the g4Rad51KR and g4Rad51KA cell lines, as previously described for the parental HEK293A7 cell line (31). To measure repair, 1×10^5 cells were plated onto a 12-well plate and transfected the next day with 0.8 μg of the I-SceI-expression vector, pCBASce (31), with 3.6 μl Lipofectamine 2000 (Invitrogen) in 1 ml of antibiotic-free medium. For the +L condition, L was added 3 h before transfection and included for the remainder experiment. Three days after transfection, GFP positive cells were quantified by flow cytometric analysis (FACS) on a Cyan ADP (Dako). Using transient transfection with a GFP expression vector and the same experimental conditions as the HDR experiments, we confirmed that the L-treated 293 cell lines have a similar transfection efficiency, as measured by the frequency of GFP^+ cells. Hence, no correction was required to determine the HDR values.

Blm depletion and immunoblot

$Blm^{tet/tet}$ cells were treated for 2 days with 1 μg/ml Doxycyclin. After 2 days, proteins were isolated by repeated freeze/thawing in NETN buffer (20 mM Tris pH8, 100 mM NaCl, 1 mM EDTA, 0.5% IGEPAL, 1 mM DTT) with Protease inhibitor cocktail (Roche). Equal amounts of total protein (15 μg) from each sample were separated on 4–12% SDS–PAGE and probed with anti-Blm antibody (ab476, Abcam) and anti-GAPDH antibody (ab9484, Abcam).

Immunofluorescence staining and time-lapse microscopy

For PICH observation, cells were fixed in 2% paraformaldehyde followed by immunostaining with anti-PICH antibody (Abnova H00054821-D01P) and Alexa fluor 568 goat anti-rabbit IgG (Invitrogen). Images were acquired using an AX-70 microscope (Olympus) equipped with a 40× NA 0.75 UPlanFl objective and a digital CCD camera (RetigaExi; QImaging). Images were collected using Image-Pro software (Media Cybernetics) for subsequent quantification. Each set of anaphases was accumulated from a number of biological replicates for each cell line ($n \geq 3$).

For real-time analysis of chromosome segregation, cells were stably transfected with pEGFP-N1-H2B (32). Time-lapse microscopy was performed using a Zeiss Observer inverted microscope equipped with a 40× NA 0.75 UPlanFl objective on cells treated for 3 days +L. Images were collected using Axiovision software (Zeiss) every 3 min for 3–6 h.

Statistical analysis

Error bars represent the standard deviation from the mean. Statistical analysis was performed using the unpaired *t*-test for HDR efficiency and clonogenic survival. The two-tailed Fisher's exact test was used for

statistical analysis of PICH–UFB, DAPI-bridge and multipolar anaphases experiments.

RESULTS

PICH–UFBs and DAPI-bridges are markers of incomplete chromosome separation in late anaphase

To investigate anaphase chromosome separation, we examined wild-type (WT) mouse ES (mES) cells using the DNA dye DAPI, as well as immunofluorescence staining to detect the helicase PICH (6,7). Using these markers, we analyzed >100 anaphases of unchallenged WT mES cells and categorized each anaphase as early or late, based on the distance between the chromosomes. From this analysis, we frequently detected PICH linkages between chromosomes in early anaphase (47%, Figure 1A and B), indicating that such linkages are a normal feature of early anaphase. In late anaphase cells, much of these PICH structures have been resolved. However, a minor fraction of late anaphases showed one or more PICH threads between chromosomes (10%, Figure 1A and B), which have been referred to as PICH–UFBs (8). We also observed a similar low frequency of late anaphases with DAPI linkages between anaphase chromosomes (7%, Figure 1A and B), which represent DAPI-bridges (33). These data indicate that a low fraction of late anaphase mES cells show evidence of incomplete chromosome separation, as detected by PICH–UFBs and DAPI-bridges.

Cells deficient in HDR, but not NHEJ, show increased levels of incomplete anaphase chromosome separation

Using PICH–UFBs and DAPI-bridges as markers, we tested whether HDR may be important for proper anaphase chromosome separation, as patients and mice with deficiencies in this pathway show elevated CIN and tumorigenesis (16). HDR involves Rad51-mediated strand exchange between sister chromatids (34). Furthermore, siRNA-depletion of Rad51 in human cells was recently shown to cause an increase in the frequency of anaphase UFBs (35). Thus, we sought to examine the effect of HDR deficiency on anaphase chromosome separation.

As Rad51 is required in vertebrates for cellular viability (36,37), we characterized a set of defined mES cell lines with non-lethal HDR deficiencies. Specifically, we examined mES-RAD51KR cells that constitutively express RAD51-K133R, which is a dominant-negative form of RAD51 that is defective for ATP-hydrolysis (26,30). In addition, we examined cells deficient in the *Brca1* and *Brca2* tumor suppressor genes, which are important for Rad51 recruitment to DNA damage and HDR (38,39). Specifically, we examined $Brca1^{11/11}$ cells that carry homozygous deletion of *Brca1* exon 11 (21) and $Brca2^{L1/L2}$ cells that have one null allele and one truncation allele of *Brca2* (25). Each of these cell lines has previously been shown to exhibit a decrease in HDR efficiency of a site-specific chromosomal DSB (22,26).

For each cell line, we analyzed more than 100 anaphase cells using the procedure described above. We found that PICH linkages were common in early anaphase cells, and the frequencies of these structures were not significantly different between HDR-deficient versus WT cells (Supplementary Figure S1A). In contrast, in late anaphase cells, we found that each HDR-deficient cell line showed a 4- to 5-fold increase in the frequency of PICH–UFBs relative to WT cells (Figure 2): WT (10%), mES-Rad51KR (41%, $P < 0.0001$), $Brca1^{11/11}$ (40%, $P < 0.0001$) $Brca2^{L1/L2}$, (52% $P < 0.0001$). These findings indicate that HDR deficiency causes incomplete anaphase chromosome separation, as detected by PICH-UFBs.

In the above experiments, we included an analysis of DAPI-bridges and found that the frequency of DAPI-bridges in late anaphase was significantly lower than PICH–UFBs in each of the cell lines. We observed a slight increase in frequency of DAPI-bridges in HDR-deficient cells, although only $Brca1^{11/11}$ cells showed a statistically significant increase in DAPI-bridges (23%, $P = 0.02$), compared to WT (7%, Figure 2). These findings indicate that late anaphase

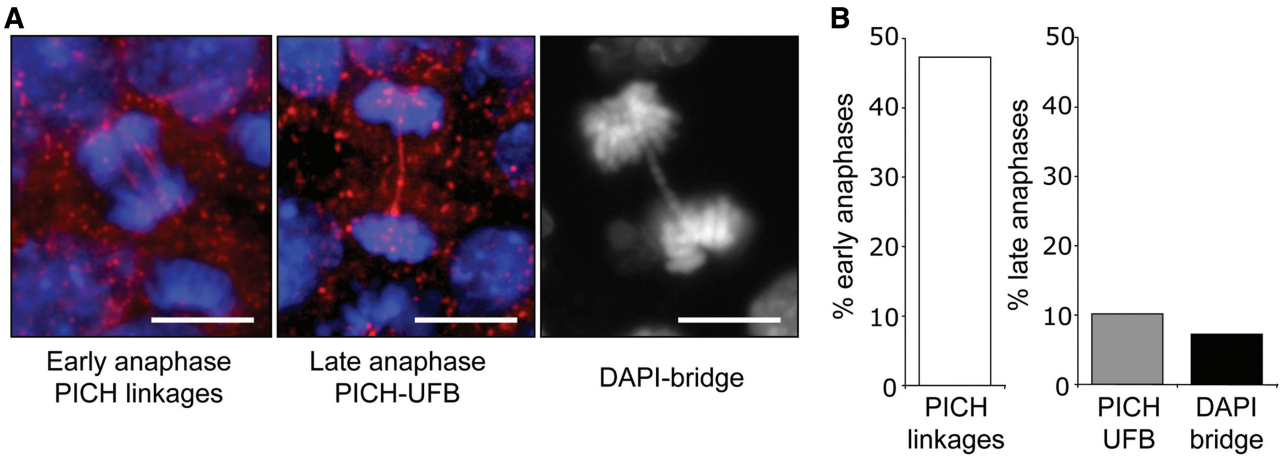

Figure 1. WT mES cells show low levels of incomplete anaphase chromosome separation. (**A**) With WT mES cells, shown are representative images of PICH linkages in early anaphase, PICH–UFBs in late anaphase and a DAPI-bridge. (**B**) Shown is the percentage of anaphases of WT mES cells with the three structures described in A.

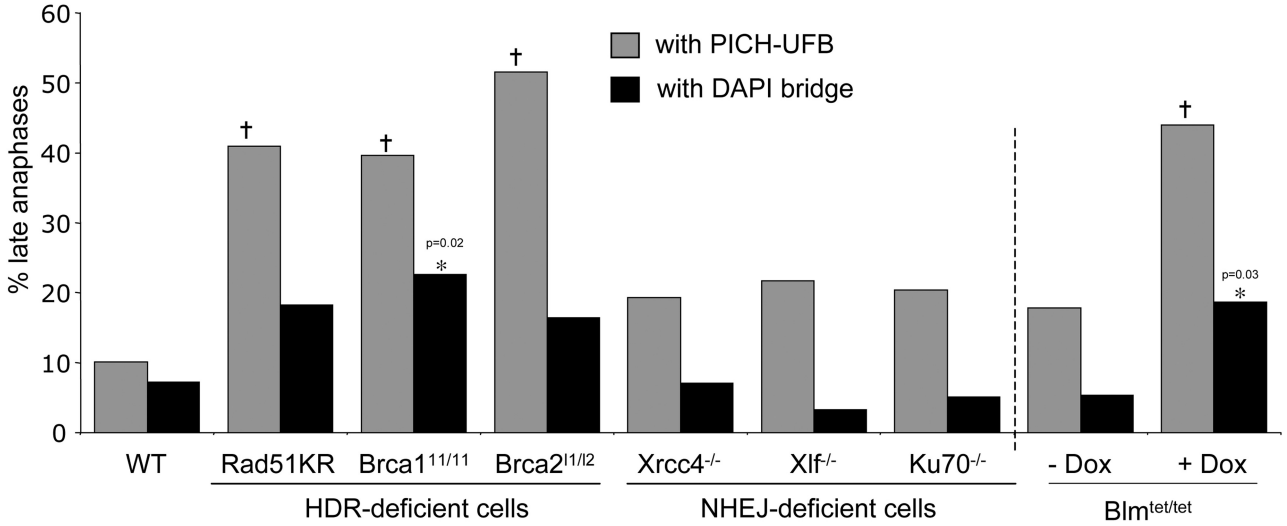

Figure 2. HDR, but not NHEJ, is important to limit PICH–UFBs. Shown is the percentage of late anaphases with PICH–UFBs (grey boxes) or DAPI-bridges (black boxes) in a set of HDR or NHEJ-deficient cell lines and a cell line enabling DOX-mediated depletion of Blm. $n > 100$ anaphases analyzed for each cell line. Dagger and Asterisk denote a difference in frequency compared to WT cells ($P < 0.002$ and $P < 0.05$, respectively). Bars, 10 μm.

PICH–UFBs are a more sensitive marker for incomplete anaphase separation caused by HDR-deficiency in mES cells, as compared to DAPI-bridges.

This accumulation of PICH–UFBs in HDR-deficient cells is similar to previous findings with human cells deficient for the BLM helicase (8). To confirm this notion in mES cells, we characterized $Blm^{tet/tet}$ mES cells (29), which enable doxycycline (DOX)-mediated Blm depletion (Supplementary Figure S1B). We found that Blm depletion caused an accumulation of late anaphase cells with PICH–UFBs (2.4-fold, $P = 0.002$, Figure 2) and DAPI-bridges (3.8-fold, $P = 0.03$, Figure 2).

As HDR is important for DSB repair (40), we considered whether another DSB repair pathway, NHEJ, might also be important for anaphase chromosome separation. For this, we analyzed anaphases of three mES cell lines with null alleles of NHEJ factors: $Xrcc4^{-/-}$, $Xlf^{-/-}$ and $Ku70^{-/-}$ (27,28,41). From these experiments, we found that loss of Xrcc4, Xlf or Ku70 did not lead to a significant increase in late anaphase PICH–UFBs or DAPI-bridges, as compared to WT cells (Figure 2). These results indicate that HDR, but not NHEJ, is important for complete anaphase chromosome separation, as measured by PICH–UFBs.

Inducible expression of two distinct dominant-negative Rad51 proteins causes different degrees of HDR disruption

We next sought to examine the effect of two different degrees of HDR disruption (i.e. mild versus severe) on anaphase chromosome separation. For this, we generated novel cell lines carrying inducible expression cassettes for two different dominant-negative Rad51 proteins: Rad51-K133R, which is defective for ATP-hydrolysis and Rad51-K133A, which is defective for ATP-binding (30). The Rad51-K133R protein shows defects in filament structural transitions during strand exchange (42), whereas the Rad51-K133A protein is inactive for filament formation (43). Accordingly, transient expression of Rad51-K133A was shown to cause a more severe disruption of HDR in mES cells, as compared to Rad51-K133R (22).

We generated clonal cell lines with stable integration of inducible expression cassettes for RAD51-K133R (g4Rad51KR) and RAD51-K133A (g4Rad51KA), using a human embryonic kidney transformed cell line (293A7). Transcription from the g4 promoter in these cassettes requires addition of a soluble L, which activates regulator proteins that are stably expressed in the 293A7 cells (Figure 3A) (44). Using quantitative RT–PCR, we confirmed L-dependent transcription of both Rad51-K133R and RAD51-K133A in the g4Rad51KR and g4Rad51KA cell lines, respectively (>20-fold at 4 h after L-addition and transcription persists for several days with continuous L-treatment), (Figure 3B).

We then determined how acute expression of these RAD51 mutants affected the efficiency of HDR and cellular viability. To examine HDR, we integrated the DR-GFP reporter into the g4Rad51KR, g4Rad51KA and parental cell lines. HDR of an I-SceI-induced DSB in DR-GFP restores a GFP cassette (22), such that HDR can be quantified as the percentage of GFP positive cells 3 days after transfection of an I-SceI expression vector. To measure cellular viability, we quantified clonogenic survival after 7 days of continuous L-treatment. As compared to the parental cell line, we found that L-treatment of the g4Rad51KR cells caused a significant, but relatively mild decrease in both HDR (1.5-fold, $P < 0.0002$, Figure 3C) and cellular viability (1.3-fold, $P = 0.0006$, Figure 3D). In contrast, L-treatment of the g4Rad51KA cells caused a more substantial decrease in both HDR efficiency (6-fold, $P < 0.0001$, Figure 3C) and cellular viability (14-fold, $P < 0.0001$, Figure 3D). These results indicate that L-treatment of g4Rad51KA cells

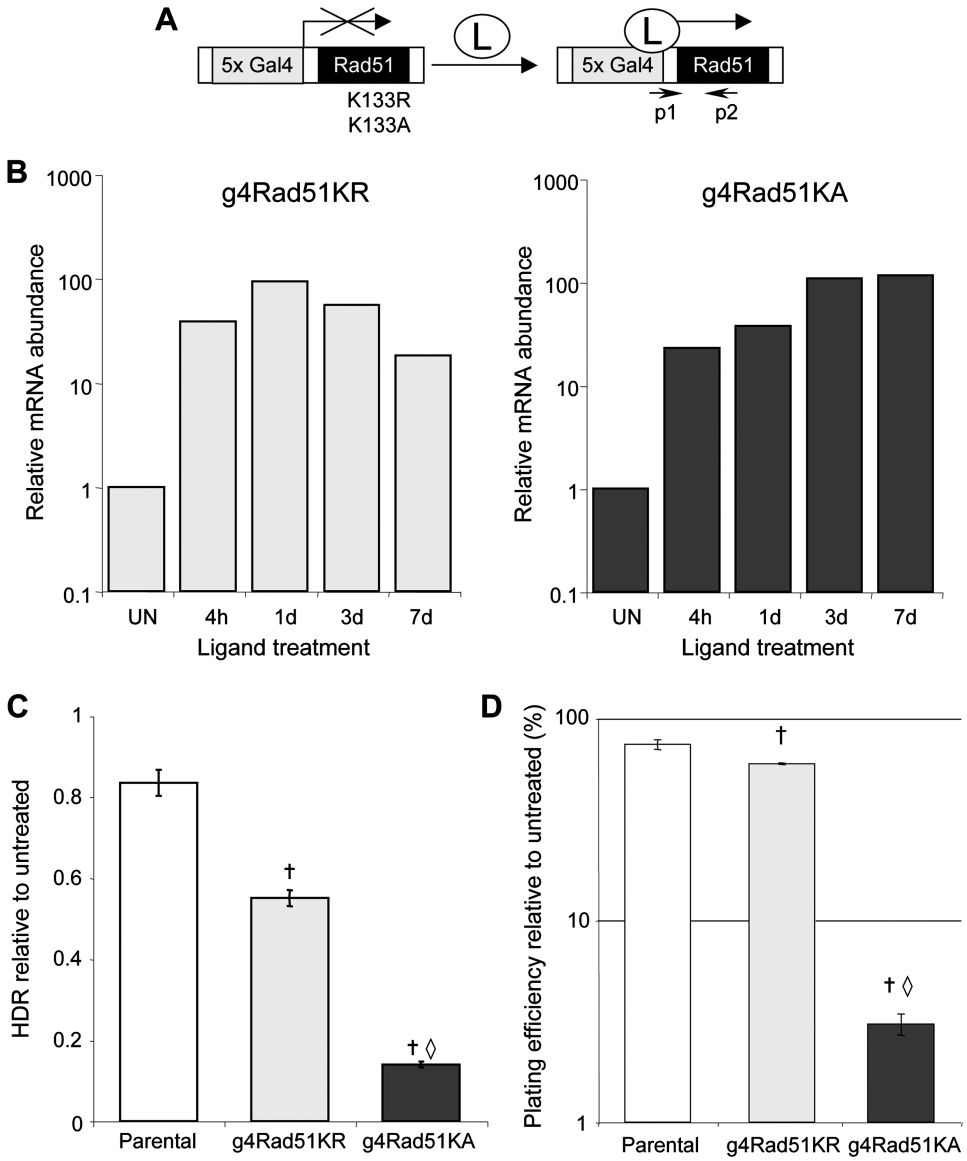

Figure 3. Inducible expression of two dominant-negative Rad51 mutants cause different degrees of HDR disruption. (**A**) Diagram shows inducible expression cassettes for Rad51-K133R and Rad51-K133A, in which transcription from the g4 promoter requires addition of the cell-permeable Genostat ligand (L). Primers p1 and p2 are used for genotyping and quantitative RT–PCR analysis. (**B**) mRNA abundance from the g4Rad51 expression cassettes, measured by quantitative RT–PCR, for the g4Rad51KR and g4Rad51KA cell lines after L-treatment for the times shown (h: hours, d: days), relative to untreated (UN). (**C**) Inducible Rad51-K133R and Rad51-K133A expression causes mild and severe HDR disruption, respectively. Shown is repair by HDR in the presence of L, relative to untreated, using the DR-GFP reporter integrated into the parental, g4Rad51KR and Rad51KA cell lines. (**D**) The degree of HDR disruption is commensurate with the effect on viability. Shown is the clonogenic survival of the cell lines in C, after continuous L-treatment. Dagger denotes a difference in frequency compared to parental cells ($P < 0.0002$). Open diamond denotes a difference of g4Rad51KA cells compared to g4Rad51KR cells ($P < 0.0001$).

causes a more severe disruption of HDR and loss of cellular viability, as compared to g4Rad51KR cells.

Severe HDR disruption causes aggravated defects in chromosome separation versus mild HDR disruption

Using these cell lines, we examined how severe versus mild disruption of HDR affects anaphase separation of chromosomes. First, we evaluated the effect of L-treatment on the frequency of PICH linkages in g4Rad51KR, g4Rad51KA and parental cell lines. The frequency of early anaphases showing PICH linkages was not different between these three cell lines and was not affected by L-treatment (Figure 4A). In contrast, in late anaphases, L-treatment of both, g4Rad51KR and g4Rad51KA caused a significant increase in PICH–UFBs (e.g. >2-fold after 3 days, $P < 0.0001$, Figure 4B). In contrast, L-treatment of the parental cells did not affect the frequency of late anaphase PICH–UFBs (Figure 4B). These results show that both, mild and severe HDR disruption causes a significant increase in PICH–UFBs in late anaphase.

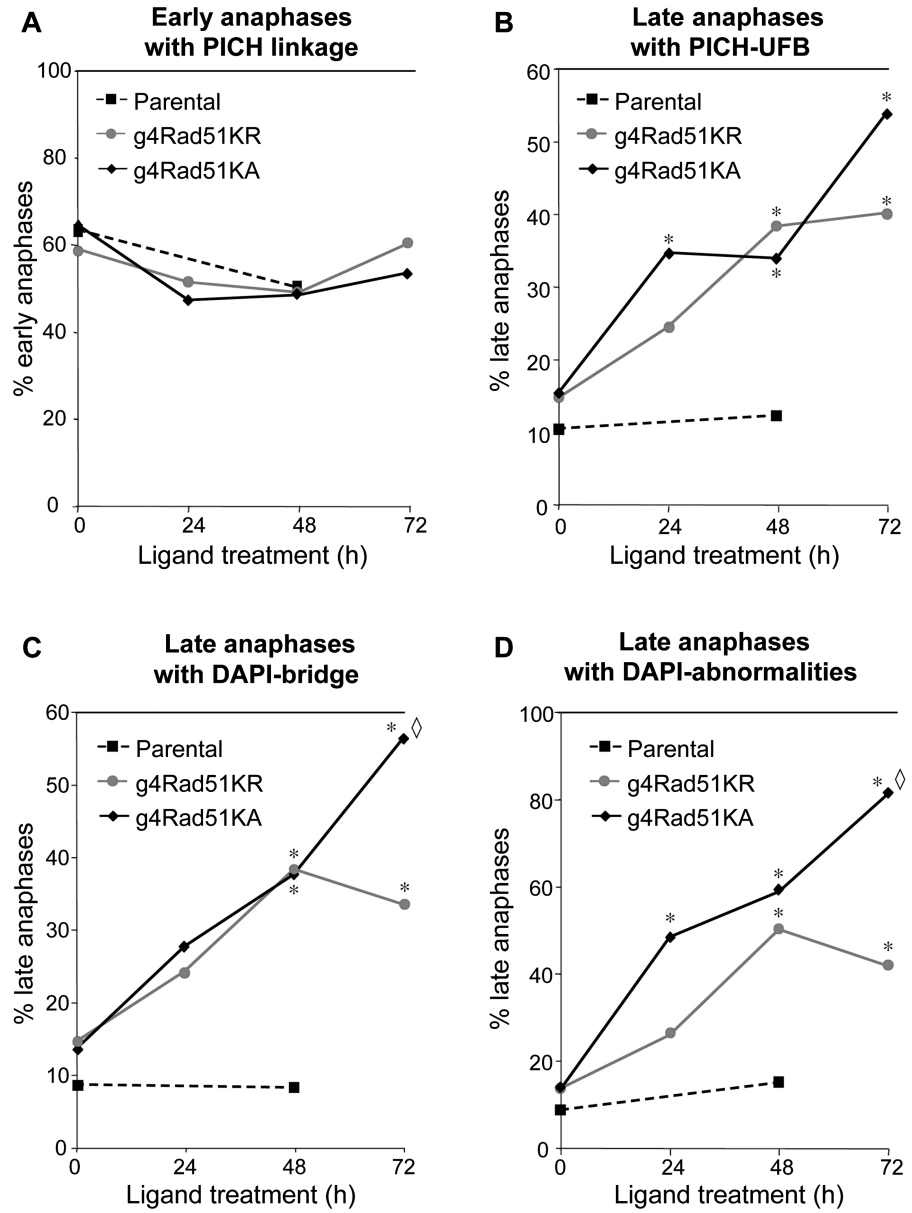

Figure 4. Mild and severe HDR disruption lead to distinct chromosome segregation defects. (**A**) Shown is the percentage of early anaphases with PICH linkages in 293A7, g4Rad51KR, g4Rad51KA cells after L-treatment. (**B**) Mild and severe HDR-deficiency causes PICH–UFBs. Shown is the percentage of late anaphases with PICH–UFBs for the cells shown in A. (**C**) As measured by DAPI, severe HDR-deficiency causes chromosome separation defects to a greater degree than a mild HDR-deficiency. Shown is the percentage of late anaphases with DAPI-bridges for the cells shown in A. (**D**) Shown is the percentage of total anaphase abnormalities (e.g. DAPI-bridges, laggards or multipolar anaphases) for the cells shown in A. $n > 100$ anaphases analyzed for each cell line. Asterisk denotes a difference in frequency compared to untreated condition ($P < 0.0003$). Open diamond denotes a difference of g4Rad51KA compared to g4Rad51KR ($P < 0.01$).

We also examined DAPI-bridges after HDR disruption. We found that 3 days of L-treatment caused an accumulation of DAPI-bridges in g4Rad51KA cells (4-fold, $P < 0.0001$) and g4Rad51KR cells (2-fold, $P < 0.0001$, Figure 4C). We also found that 3 days of L-treatment caused an overall increase in DAPI-stained anaphase abnormalities (e.g. laggards, chromatin bridges or multipolar anaphases) in both the g4Rad51KA and g4Rad51KR cells (6-fold and 3-fold, respectively, $P < 0.0001$, Figure 4D). Based on the cellular doubling times of these cell lines in the presence of L (g4Rad51KA 30 h, g4Rad51KR 24 h and parental 21 h, see 'Materials and Methods' section), the 3-day L-treatment reflects an average of 2.4 and 3 cell divisions for the g4Rad51KA and g4Rad51KR cell lines, respectively. Notably, after 3 days of L-treatment of g4Rad51KA cells, nearly all of the anaphases showed a chromosome separation defect as measured by DAPI (81% of late anaphases, Figure 4D). Importantly, these chromosome separation defects were significantly lower in g4Rad51KR cells, compared to g4Rad51KA cells (DAPI-bridges, 1.7-fold lower, $P = 0.01$, Figure 4C; overall DAPI abnormalities, 2-fold lower, $P < 0.0001$, Figure 4D). These findings indicate that

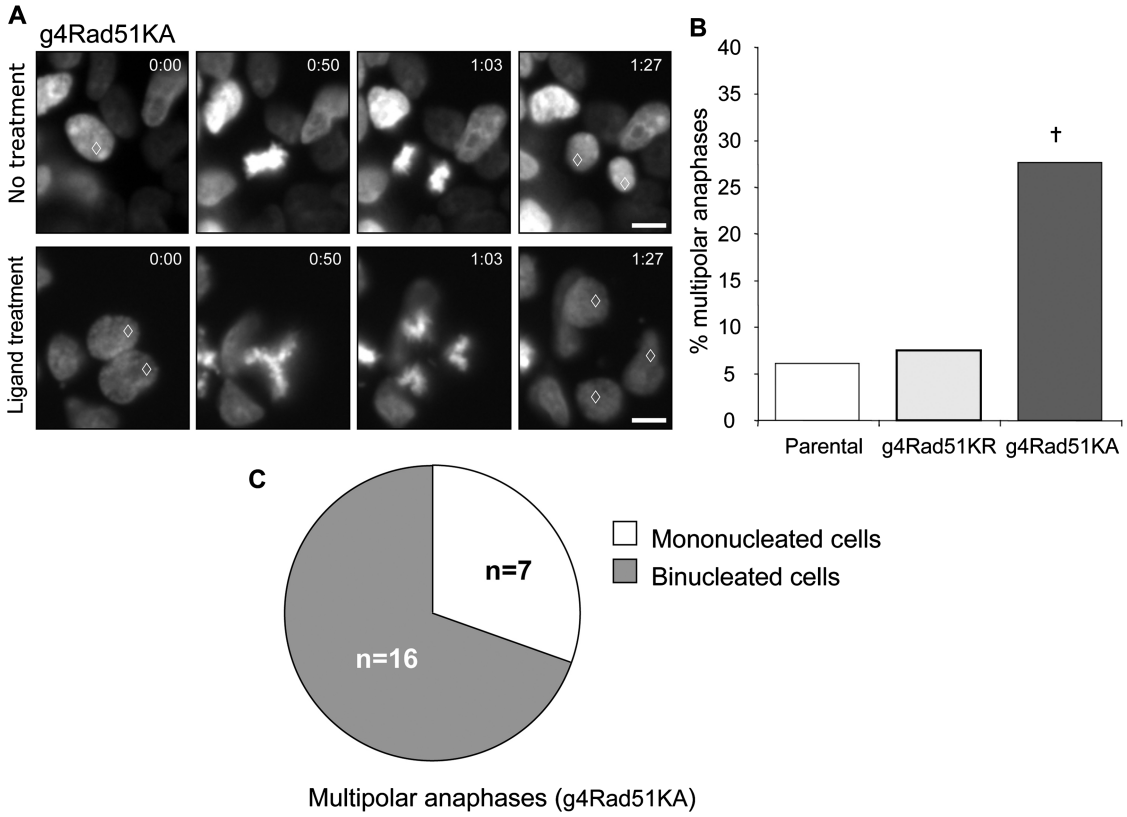

Figure 5. Severe HDR deficiency causes multipolar anaphases. (**A**) Representative time-lapse pictures from real-time imaging of cells expressing H2B-GFP. Top panel shows a normal mitosis from untreated cells. Bottom panel shows a binucleated g4Rad51KA cell resulting in a multipolar anaphase after L-treatment. Time of acquisition is in minutes. Open diamond denotes nuclei involved in observed mitosis. (**B**) Severe HDR-deficiency causes multipolar anaphases. Shown is the frequency of multipolar anaphases in 293A7, g4Rad51KR, g4Rad51KA after a 3-day L-treatment. $n > 200$ anaphases analyzed for each cell line. (**C**) Multipolar anaphases originate from binucleated cells. Diagram shows distribution of multipolar anaphase originating from single nucleated cells or binucleated cells after a 3-day L-treatment in g4Rad51KA cells. Dagger denotes a difference in frequency compared to the 293A7 cell line ($P < 0.0001$). Bars, 10 μm.

anaphase defects as measured by DAPI are induced to a greater degree following severe versus mild HDR disruption.

To further examine how the severity of HDR disruption affects anaphase progression, we monitored chromosome segregation in live cells after 3 days of L-treatment. For this, we established parental, g4Rad51KR and g4Rad51KA cell lines stably expressing the histone H2B–GFP fusion protein, which enables chromatin visualization (32). In this experiment, L-treated parental and g4Rad51KR cells showed mostly bipolar anaphases that resolve into two distinct daughter cells (Figure 5A, Supplementary Video 1) and a low frequency of multipolar anaphases (7% and 6%, respectively, Figure 5B). However, L-treated g4Rad51KA cells showed a high frequency of multipolar anaphases (28%, Figure 5A and B, Supplementary Figure S1C and Supplementary Video 2). These results indicate that severe HDR disruption causes an accumulation of multipolar anaphases, whereas mild HDR disruption has no consequence on anaphase polarity.

We next examined the sequence of events leading to multipolar anaphases in the g4Rad51KA cells. Using extended time-lapse microscopy, we found that the majority of multipolar anaphases originated from binucleated cells (70%, $n = 23$, Figure 5A and C, Supplementary Video 2), which likely arise from a previous mitotic separation defect (45). These results indicate that severe HDR disruption leads to binucleated cells that subsequently undergo a multipolar division, which has been shown to be a lethal chromosome segregation event (4).

DISCUSSION

Multiple HDR factors, but not NHEJ, are important to limit PICH–UFBs

We have presented evidence that disruption of HDR, but not NHEJ, causes incomplete anaphase chromosome separation. As both HDR and NHEJ are important for DSB repair, this finding indicates that the anaphase abnormalities in HDR-deficient cells may not be caused by inefficient DSB repair. Rather, HDR-deficient cells may fail to restart stalled or blocked replication forks (46,47) and thereby accumulate unreplicated regions, which have been proposed to cause UFBs (48). Consistent with this notion, HDR-deficient cells show defects in replication progression (49,50) and inhibitors of replicative DNA polymerases cause incomplete

anaphase chromosome separation, as measured by UFBs (12). Similarly, incomplete replication of rDNA and telomere loci, caused by disruption of cohesin complexes and telomere sheltering factors, respectively, each leads to abnormal chromosome segregation (51,52). In summary, we suggest that the role of HDR during DNA replication is critical to limit incomplete chromosome separation during anaphase.

A number of cell lines that are deficient in distinct steps of HDR each showed elevated levels of PICH–UFBs. To begin with, Brca2 directly interacts with Rad51 to promote strand exchange (53,54). As well, Brca2, like Rad51, is important to promote HDR and inhibit another homologous repair pathway, single-strand annealing (SSA) (22). In contrast, Brca1 likely functions at the earlier step of end resection, as Brca1 promotes both HDR and SSA (22) and is important for ssDNA formation (55). Furthermore, the Rad51-K133R and Rad51-K133A proteins likely affect HDR via distinct mechanisms. Namely, Rad51-K133R affects filament structural transitions during strand exchange and hence, may disrupt HDR by preventing Rad51 dissociation from the DNA after filament formation (42). In contrast, the Rad51-K133A protein is defective for DNA binding and strand exchange (43) and hence, may disrupt HDR by interacting with WT Rad51 to block DNA binding. Finally, the Blm helicase appears to play a role in multiple aspects of genome maintenance (56,57), including the resolution of HDR intermediates, since BLM-deficient cells show elevated sister chromatid exchanges and allelic crossover recombination (29). Notably, since disruption of either BLM or Rad51 causes elevated frequencies of PICH–UFBs, we posit that the role of BLM during HDR may be linked to its requirement for limiting PICH–UFBs. Alternatively, since decatenation stress also leads to PICH–UFBs (6–8), BLM and other HDR factors could potentially also play a role in chromosome decatenation. In any case, our finding that disruption of each of these factors causes a similar increase in PICH–UFBs indicates that multiple steps of HDR are essential for complete anaphase chromosome separation.

Severe and mild HDR disruption cause distinct anaphase separation defects, with implications for cell viability and CIN

We have presented evidence that a severe HDR disruption (expression of Rad51-K133A) leads to inviable cells, along with massive chromosome separation defects, as detected by PICH–UFBs and DAPI-abnormalities. In addition, severe HDR disruption caused multipolar anaphases, which could directly result from a failure to resolve the anaphase linkages that are detected by PICH and/or DAPI. Alternatively, these multipolar anaphases could arise independently from the anaphase linkages. Consistent with the former model, these multipolar anaphases largely arose from binucleated cells, which likely result from prior anaphase chromosome separation defects (45). As it was recently shown that multipolar divisions lead to inviable cells (4), we suggest that the multipolar divisions caused by severe HDR disruption contribute to the observed loss of cell viability.

In contrast, we found that mild HDR disruption causes viable chromosome separation defects, namely, mild HDR disruption (expression of Rad51-K133R) led to a similar increase in PICH–UFBs compared to severe HDR disruption and to a moderate increase in DAPI-bridges. Cells with such a significant frequency of incomplete chromosome separation during anaphase are likely prone to substantial CIN, since unresolved PICH–UFBs in late anaphase could be fragmented during cytokinesis (7,8). Consistent with this notion, HDR deficient cells have increased CIN as determined by aneuploidy and the high frequency of micronuclei (18,58). However, we found that mild HDR disruption does not result in multipolar divisions, but maintains bipolar chromosome segregation, which favors cell viability (4).

Based on these findings, we propose a model whereby, mild HDR deficiency promotes the proliferation of cells prone to CIN due to chromosome separation defects, whereas, severe HDR deficiency results in multipolar anaphases associated with cell death (Figure 6). Accordingly, severe deficiencies in HDR genes (e.g. *Brca1* and *Brca2*) might lead to efficient cell death, whereas milder alleles could cause CIN and cell survival, thus contributing to tumorigenesis (59,60). Notably, since HDR deficiency may be prevalent for some tumor types (61), we suggest that examining the severity of HDR disruption of individual tumors, including the relative consequences on

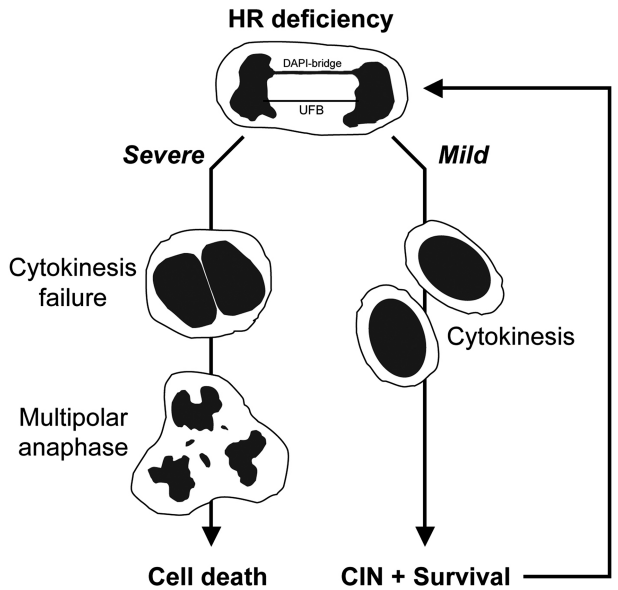

Figure 6. Model for consequences of mild versus severe HDR disruption on anaphase and cell viability. Both severe and mild HDR deficiencies lead to incomplete chromosome separation, as measured by PICH–UFBs (red) and DAPI bridges (blue). Cells with a mild HDR deficiency retain bipolar chromosome separation and viability, but are incapable of limiting anaphase abnormalities and hence are prone to CIN. In contrast, severe HDR deficiency additionally causes multipolar anaphases resulting mostly from binucleated cells and eventual cell death.

anaphase chromosome separation, will provide insight into the etiology and treatment of such cancers.

SUPPLEMENTARY DATA

Supplementary Data are available at NAR Online.

ACKNOWLEDGEMENTS

We thank Dr G.M. Wahl for the H2B-GFP plasmid and the BRI/COH Light Microscopy Core for assistance.

FUNDING

Funding for open access charge: The National Cancer Institute of the National Institutes of Health, grant RO1CA120954 (to J.M.S.).

REFERENCES

1. Nasmyth,K. (2002) Segregating sister genomes: the molecular biology of chromosome separation. *Science*, **297**, 559–565.
2. Nitiss,J.L. (2009) DNA topoisomerase II and its growing repertoire of biological functions. *Nat. Rev. Cancer*, **9**, 327–337.
3. Ishida,R., Sato,M., Narita,T., Utsumi,K.R., Nishimoto,T., Morita,T., Nagata,H. and Andoh,T. (1994) Inhibition of DNA topoisomerase II by ICRF-193 induces polyploidization by uncoupling chromosome dynamics from other cell cycle events. *J. Cell Biol.*, **126**, 1341–1351.
4. Ganem,N.J., Godinho,S.A. and Pellman,D. (2009) A mechanism linking extra centrosomes to chromosomal instability. *Nature*, **460**, 278–282.
5. Ishida,R., Miki,T., Narita,T., Yui,R., Sato,M., Utsumi,K.R., Tanabe,K. and Andoh,T. (1991) Inhibition of intracellular topoisomerase II by antitumor bis(2,6-dioxopiperazine) derivatives: mode of cell growth inhibition distinct from that of cleavable complex-forming type inhibitors. *Cancer Res.*, **51**, 4909–4916.
6. Baumann,C., Korner,R., Hofmann,K. and Nigg,E.A. (2007) PICH, a Centromere-Associated SNF2 Family ATPase, is regulated by Plk1 and required for the spindle checkpoint. **128**, 101–114.
7. Wang,L.H., Schwarzbraun,T., Speicher,M.R. and Nigg,E.A. (2008) Persistence of DNA threads in human anaphase cells suggests late completion of sister chromatid decatenation. *Chromosoma*, **117**, 123–135.
8. Chan,K.L., North,P.S. and Hickson,I.D. (2007) BLM is required for faithful chromosome segregation and its localization defines a class of ultrafine anaphase bridges. *Embo J.*, **26**, 3397–3409.
9. German,J., Crippa,L.P. and Bloom,D. (1974) Bloom's syndrome. III. Analysis of the chromosome aberration characteristic of this disorder. *Chromosoma*, **48**, 361–366.
10. Bartram,C.R., Koske-Westphal,T. and Passarge,E. (1976) Chromatid exchanges in ataxia telangiectasia, Bloom syndrome, Werner syndrome, and xeroderma pigmentosum. *Ann. Hum. Genet.*, **40**, 79–86.
11. Moldovan,G.L. and D'Andrea,A.D. (2009) How the fanconi anemia pathway guards the genome. *Annu. Rev. Genet.*, **43**, 223–249.
12. Chan,K.L., Palmai-Pallag,T., Ying,S. and Hickson,I.D. (2009) Replication stress induces sister-chromatid bridging at fragile site loci in mitosis. *Nat. Cell Biol.*, **11**, 753–760.
13. Vinciguerra,P., Godinho,S.A., Parmar,K., Pellman,D. and D'Andrea,A.D. (2010) Cytokinesis failure occurs in Fanconi anemia pathway-deficient murine and human bone marrow hematopoietic cells. *J. Clin. Invest.*, **120**, 3834–3842.
14. Naim,V. and Rosselli,F. (2009) The FANC pathway and BLM collaborate during mitosis to prevent micro-nucleation and chromosome abnormalities. *Nat. Cell Biol.*, **11**, 761–768.
15. Moynahan,M.E. and Jasin,M. (2010) Mitotic homologous recombination maintains genomic stability and suppresses tumorigenesis. *Nat. Rev. Mol. Cell Biol.*, **11**, 196–207.
16. Pierce,A.J., Stark,J.M., Araujo,F.D., Moynahan,M.E., Berwick,M. and Jasin,M. (2001) Double-strand breaks and tumorigenesis. *Trends Cell Biol.*, **11**, S52–S59.
17. Kraakman-van der Zwet,M., Overkamp,W.J., van Lange,R.E., Essers,J., van Duijn-Goedhart,A., Wiggers,I., Swaminathan,S., van Buul,P.P., Errami,A., Tan,R.T. *et al.* (2002) Brca2 (XRCC11) deficiency results in radioresistant DNA synthesis and a higher frequency of spontaneous deletions. *Mol. Cell. Biol.*, **22**, 669–679.
18. Daboussi,F., Thacker,J. and Lopez,B.S. (2005) Genetic interactions between RAD51 and its paralogues for centrosome fragmentation and ploidy control, independently of the sensitivity to genotoxic stresses. *Oncogene*, **24**, 3691–3696.
19. Starita,L.M., Machida,Y., Sankaran,S., Elias,J.E., Griffin,K., Schlegel,B.P., Gygi,S.P. and Parvin,J.D. (2004) BRCA1-dependent ubiquitination of gamma-tubulin regulates centrosome number. *Mol. Cell. Biol.*, **24**, 8457–8466.
20. Dodson,H., Bourke,E., Jeffers,L.J., Vagnarelli,P., Sonoda,E., Takeda,S., Earnshaw,W.C., Merdes,A. and Morrison,C. (2004) Centrosome amplification induced by DNA damage occurs during a prolonged G2 phase and involves ATM. *EMBO J.*, **23**, 3864–3873.
21. Moynahan,M.E., Chiu,J.W., Koller,B.H. and Jasin,M. (1999) Brca1 controls homology-directed DNA repair. *Mol. Cell*, **4**, 511–518.
22. Stark,J.M., Pierce,A.J., Oh,J., Pastink,A. and Jasin,M. (2004) Genetic steps of mammalian homologous repair with distinct mutagenic consequences. *Mol. Cell. Biol.*, **24**, 9305–9316.
23. Richardson,C., Stark,J.M., Ommundsen,M. and Jasin,M. (2004) Rad51 overexpression promotes alternative double-strand break repair pathways and genome instability. *Oncogene*, **23**, 546–553.
24. Daniels,M.J., Wang,Y., Lee,M. and Venkitaraman,A.R. (2004) Abnormal cytokinesis in cells deficient in the breast cancer susceptibility protein BRCA2. *Science*, **306**, 876–879.
25. Morimatsu,M., Donoho,G. and Hasty,P. (1998) Cells deleted for Brca2 COOH terminus exhibit hypersensitivity to gamma-radiation and premature senescence. *Cancer Res.*, **58**, 3441–3447.
26. Stark,J.M., Hu,P., Pierce,A.J., Moynahan,M.E., Ellis,N. and Jasin,M. (2002) ATP hydrolysis by mammalian RAD51 has a key role during homology-directed DNA repair. *J. Biol. Chem.*, **277**, 20185–20194.
27. Gao,Y., Sun,Y., Frank,K.M., Dikkes,P., Fujiwara,Y., Seidl,K.J., Sekiguchi,J.M., Rathbun,G.A., Swat,W., Wang,J. *et al.* (1998) A critical role for DNA end-joining proteins in both lymphogenesis and neurogenesis. *Cell*, **95**, 891–902.
28. Zha,S., Alt,F.W., Cheng,H.L., Brush,J.W. and Li,G. (2007) Defective DNA repair and increased genomic instability in Cernunnos-XLF-deficient murine ES cells. *Proc. Natl Acad. Sci. USA*, **104**, 4518–4523.
29. Yusa,K., Horie,K., Kondoh,G., Kouno,M., Maeda,Y., Kinoshita,T. and Takeda,J. (2004) Genome-wide phenotype analysis in ES cells by regulated disruption of Bloom's syndrome gene. *Nature*, **429**, 896–899.
30. Morrison,C., Shinohara,A., Sonoda,E., Yamaguchi-Iwai,Y., Takata,M., Weichselbaum,R.R. and Takeda,S. (1999) The essential functions of human Rad51 are independent of ATP hydrolysis. *Mol. Cell. Biol.*, **19**, 6891–6897.
31. Bennardo,N., Cheng,A., Huang,N. and Stark,J.M. (2008) Alternative-NHEJ is a mechanistically distinct pathway of mammalian chromosome break repair. *PLoS Genet.*, **4**, e1000110.
32. Kanda,T., Sullivan,K.F. and Wahl,G.M. (1998) Histone-GFP fusion protein enables sensitive analysis of chromosome dynamics in living mammalian cells. *Curr. Biol.*, **8**, 377–385.
33. Gisselsson,D. (2005) Mitotic instability in cancer: is there method in the madness? *Cell Cycle*, **4**, 1007–1010.
34. Sung,P., Krejci,L., Van Komen,S. and Sehorn,M.G. (2003) Rad51 recombinase and recombination mediators. *J. Biol. Chem.*, **278**, 42729–42732.
35. LahkimBennani-Belhaj,K., Rouzeau,S., Buhagiar-Labarchede,G., Chabosseau,P., Onclercq-Delic,R., Bayart,E., Cordelieres,F., Couturier,J. and Amor-Gueret,M. (2010) The Bloom syndrome

protein limits the lethality associated with RAD51 deficiency. *Mol. Cancer Res.*, **8**, 385–394.
36. Lim,D.S. and Hasty,P. (1996) A mutation in mouse rad51 results in an early embryonic lethal that is suppressed by a mutation in p53. *Mol. Cell. Biol.*, **16**, 7133–7143.
37. Tsuzuki,T., Fujii,Y., Sakumi,K., Tominaga,Y., Nakao,K., Sekiguchi,M., Matsushiro,A., Yoshimura,Y. and Morita,T. (1996) Targeted disruption of the Rad51 gene leads to lethality in embryonic mice. *Proc. Natl Acad. Sci. USA*, **93**, 6236–6240.
38. Jasin,M. (2002) Homologous repair of DNA damage and tumorigenesis: the BRCA connection. *Oncogene*, **21**, 8981–8993.
39. Scully,R. and Livingston,D.M. (2000) In search of the tumour-suppressor functions of BRCA1 and BRCA2. *Nature*, **408**, 429–432.
40. Kass,E.M. and Jasin,M. (2010) Collaboration and competition between DNA double-strand break repair pathways. *FEBS Lett.*, **584**, 3703–3708.
41. Gu,Y., Jin,S., Gao,Y., Weaver,D.T. and Alt,F.W. (1997) Ku70-deficient embryonic stem cells have increased ionizing radiosensitivity, defective DNA end-binding activity, and inability to support V(D)J recombination. *Proc. Natl Acad. Sci. USA*, **94**, 8076–8081.
42. Robertson,R.B., Moses,D.N., Kwon,Y., Chan,P., Chi,P., Klein,H., Sung,P. and Greene,E.C. (2009) Structural transitions within human Rad51 nucleoprotein filaments. *Proc. Natl Acad. Sci. USA*, **106**, 12688–12693.
43. Chi,P., Van Komen,S., Sehorn,M.G., Sigurdsson,S. and Sung,P. (2006) Roles of ATP binding and ATP hydrolysis in human Rad51 recombinase function. *DNA Repair (Amst)*, **5**, 381–391.
44. Palli,S.R., Kapitskaya,M.Z., Kumar,M.B. and Cress,D.E. (2003) Improved ecdysone receptor-based inducible gene regulation system. *Eur. J. Biochem.*, **270**, 1308–1315.
45. Ganem,N.J., Storchova,Z. and Pellman,D. (2007) Tetraploidy, aneuploidy and cancer. *Curr. Opin. Genet. Dev.*, **17**, 157–162.
46. Petermann,E. and Helleday,T. (2010) Pathways of mammalian replication fork restart. *Nat. Rev. Mol. Cell Biol.*, **11**, 683–687.
47. Allen,C., Ashley,A.K., Hromas,R. and Nickoloff,J.A. (2011) More forks on the road to replication stress recovery. *J. Mol. Cell Biol.*, **3**, 4–12.
48. Chan,K.L. and Hickson,I.D. (2009) On the origins of ultra-fine anaphase bridges. *Cell Cycle*, **8**, 3065–3066.
49. Daboussi,F., Courbet,S., Benhamou,S., Kannouche,P., Zdzienicka,M.Z., Debatisse,M. and Lopez,B.S. (2008) A homologous recombination defect affects replication-fork progression in mammalian cells. *J. Cell Sci.*, **121**, 162–166.
50. Sonoda,E., Sasaki,M.S., Buerstedde,J.M., Bezzubova,O., Shinohara,A., Ogawa,H., Takata,M., Yamaguchi-Iwai,Y. and Takeda,S. (1998) Rad51-deficient vertebrate cells accumulate chromosomal breaks prior to cell death. *EMBO J.*, **17**, 598–608.
51. Torres-Rosell,J., De Piccoli,G., Cordon-Preciado,V., Farmer,S., Jarmuz,A., Machin,F., Pasero,P., Lisby,M., Haber,J.E. and Aragon,L. (2007) Anaphase onset before complete DNA replication with intact checkpoint responses. *Science*, **315**, 1411–1415.
52. Sfeir,A., Kosiyatrakul,S.T., Hockemeyer,D., MacRae,S.L., Karlseder,J., Schildkraut,C.L. and de Lange,T. (2009) Mammalian telomeres resemble fragile sites and require TRF1 for efficient replication. *Cell*, **138**, 90–103.
53. Liu,J., Doty,T., Gibson,B. and Heyer,W.D. (2010) Human BRCA2 protein promotes RAD51 filament formation on RPA-covered single-stranded DNA. *Nat. Struct. Mol. Biol.*, **17**, 1260–1262.
54. Jensen,R.B., Carreira,A. and Kowalczykowski,S.C. (2010) Purified human BRCA2 stimulates RAD51-mediated recombination. *Nature*, **467**, 678–683.
55. Schlegel,B.P., Jodelka,F.M. and Nunez,R. (2006) BRCA1 promotes induction of ssDNA by ionizing radiation. *Cancer Res.*, **66**, 5181–5189.
56. Bugreev,D.V., Yu,X., Egelman,E.H. and Mazin,A.V. (2007) Novel pro- and anti-recombination activities of the Bloom's syndrome helicase. *Genes Dev.*, **21**, 3085–3094.
57. Sung,P. and Klein,H. (2006) Mechanism of homologous recombination: mediators and helicases take on regulatory functions. *Nat. Rev. Mol. Cell Biol.*, **7**, 739–750.
58. Ban,S., Shinohara,T., Hirai,Y., Moritaku,Y., Cologne,J.B. and MacPhee,D.G. (2001) Chromosomal instability in BRCA1- or BRCA2-defective human cancer cells detected by spontaneous micronucleus assay. *Mutat. Res.*, **474**, 15–23.
59. Elledge,S.J. and Amon,A. (2002) The BRCA1 suppressor hypothesis: an explanation for the tissue-specific tumor development in BRCA1 patients. *Cancer Cell*, **1**, 129–132.
60. Sherr,C.J. (2004) Principles of tumor suppression. *Cell*, **116**, 235–246.
61. Konstantinopoulos,P.A., Spentzos,D., Karlan,B.Y., Taniguchi,T., Fountzilas,E., Francoeur,N., Levine,D.A. and Cannistra,S.A. (2010) Gene expression profile of BRCAness that correlates with responsiveness to chemotherapy and with outcome in patients with epithelial ovarian cancer. *J. Clin. Oncol.*, **28**, 3555–3561.